Osteoblastic Phenotype Expression of MC3T3-E1 Cultured on Electrospun Polycaprolactone Fiber Mats Filled with Hydroxyapatite Nanoparticles

3 AUTHORS:

Patcharaporn Wutticharoenmongkol
Thammasat University
8 PUBLICATIONS **465** CITATIONS

SEE PROFILE

Prasit Pavasant
Chulalongkorn University
129 PUBLICATIONS **1,833** CITATIONS

SEE PROFILE

Pitt Supaphol
Chulalongkorn University
234 PUBLICATIONS **6,417** CITATIONS

SEE PROFILE

Osteoblastic Phenotype Expression of MC3T3-E1 Cultured on Electrospun Polycaprolactone Fiber Mats Filled with Hydroxyapatite Nanoparticles

Patcharaporn Wutticharoenmongkol,[†] Prasit Pavasant,[‡] and Pitt Supaphol*,[†]

Technological Center for Electrospun Fibers and The Petroleum and Petrochemical College and Department of Anatomy, Faculty of Dentistry, Chulalongkorn University, Phyathai Road, Pathumwan, Bangkok 10330, Thailand

Electrospun (e-spun) fiber mats of polycaprolactone (PCL; $M_n = 80\,000$ g mol^{-1}) with or without the presence of hydroxyapatite (HAp) nanoparticles (at 1% w/v based on the volume of the PCL solution) were successfully fabricated. The potential for use of these e-spun fiber mats as bone scaffolds was assessed by mouse calvaria-derived pre-osteoblastic cells, MC3T3-E1, in terms of attachment, proliferation, differentiation, and mineralization. Despite the lower number of cells attached at early time points, both the fibrous scaffolds supported the proliferation of MC3T3-E1 at similar levels to tissue-culture polystyrene plate (TCPS), with the cells growing on the PCL/HAp fiber mat (i.e., PCL/HAp-FS) showing the greatest proliferation rate on day 3 after the initial attachment period of 16 h. Alkaline phosphatase (ALP) activity of the cells grown on TCPS was the greatest on day 3 after cell culturing, while that of the cells grown on PCL/HAp-FS reached a maximum on day 5. On the other hand, the ALP activity of the cells grown on the neat PCL fiber mat (i.e., PCL-FS) was the lowest at any given time point. MC3T3-E1 cultured on the surface of PCL/HAp-FS expressed the greatest amount of osteocalcin (OC) gene on day 14 after cell culturing and OC protein on day 21 after cell culturing, respectively, when compared with those cultured on the surfaces of PCL-FS and TCPS. This corresponded to the greatest extent of mineralization for the cells grown on the surface of PCL/HAp-FS on day 21, followed by that for the cells grown on PCL-FS and TCPS, respectively.

1. Introduction

Electrospinning (e-spinning) is a process by which ultrafine fibers with diameters of individual fibers in the sub-micrometer down to nanometer range can be fabricated.[1,2] This process involves the application of a high electrical potential from a high-voltage power supply to a polymer liquid (i.e., solution or melt) across a finite distance between a conductive capillary and a grounded collecting device. The Coulombic repulsion force between charges of the same polarity in the polymer liquid destabilizes the partially spherical droplet of the polymer liquid located at the tip of the capillary to finally form a droplet with a conical shape (i.e., the Taylor cone). A further increase in the electrostatic field strength beyond a critical value causes an ejection of a charged stream of the polymer liquid (i.e., the charged jet) from the apex of the cone. Finally, ultrafine fibers, usually as a non-woven fiber mat, were collected on the collector. Because of their physical uniqueness (e.g., a high surface area to mass or volume ratio, a small inter-fibrous pore size with a high porosity of the obtained fiber mat, vast possibilities for surface functionalization, etc.), the proposed use for electrospun (e-spun) polymeric fibers is in areas such as filters,[3] composite reinforcements,[4,5] carriers for topical or transdermal delivery of drugs,[6,7] and scaffolds for cell and tissue cultures.[8–15]

The challenge in tissue engineering is the design of scaffolds that can mimic the structure and biological functions of the natural extracellular matrix (ECM).[8–10] The important aspects of e-spun fibers as tissue-engineered scaffolds are the three-dimensional structure with interconnected pores and high porosity that resembles fibrous collagen in the natural ECM. The most commonly used biodegradable, synthetic polymers are polylactide (PLA), polyglycolide (PGA), polycaprolactone (PCL), and their corresponding copolymers.[16–18] PCL, due to its slow in vivo degradation,[19] is a good candidate for further fabrication into a bone scaffold. To improve both the mechanical properties and the osteoconductivity of PCL scaffolds, rigid hydroxyapatite (HAp), a synthetic calcium phosphate ceramic that mimics the natural apatite composition of bone and teeth, is often used as a reinforcing bioactive agent.[20,21]

Previously, successful fabrication of e-spun PCL fiber mats containing calcium carbonate (CaCO$_3$) or HAp nanoparticles was reported.[22] The potential use of these fiber mats as bone scaffolds was first assessed by an indirect cytotoxicity evaluation with human osteogenic sarcoma cells (SaOS-2) and mouse fibroblastic cells (L929). The results suggested a high potential for use of these fiber mats as bone scaffolds, as they were posed as nontoxic to the cells. These e-spun fiber mats as bone scaffolds were further evaluated in vitro with SaOS-2 in terms of the attachment, proliferation, and alkaline phosphatase (ALP) activity of the cells that were cultured directly on the scaffolds,[11] in comparison to those of the cells on the corresponding solvent-cast films and a tissue-culture polystyrene plate (TCPS). All of the fiber mats showed much better adhesion and proliferation of the cells than the corresponding films and TCPS. The majority of the cells on all of the fibrous scaffolds was well-expanded with evidence of filopodia (i.e., slender cytoplasmic projections extending from the leading edge of the migrating cells[26] that

* Corresponding author. E-mail: pitt.s@chula.ac.th.
† Technological Center for Electrospun Fibers and The Petroleum and Petrochemical College.
‡ Department of Anatomy, Faculty of Dentistry.

help the cells during their migration over the surface of a scaffold) and attached on the fiber surface very well even at 1 h after cell seeding, while the majority of the cells on all of the film scaffolds and the glass substrate remained rounded. Among the various fibrous scaffolds investigated, the one that was filled with 1.0 wt % HAp (i.e., PCL/1.0HAp) showed the highest ALP activity.

Osteoblast-like cells exhibited differing rates of mineralization when grown on different polymer surfaces.[23,24] In their first report, Calvert et al.[23] evaluated the ability of two common biodegradable, synthetic polyesters (i.e., PCL and poly(lactide-*co*-glycolide) (PLGA)), as well as some of their blends in the form of thin films in supporting proliferation and differentiation of bone marrow stromal cells. They found that, at the end of 2 weeks after cell culturing, while there was no statistical difference in the proliferation rate of the cells on any substrate, PCL was the only material that showed negative staining for alkaline phosphatase and calcification activities.[23] Working on a different cell line (mouse calvaria-derived, pre-osteoblastic cells, MC3T3-E1), Calvert et al.[24] showed in their subsequent report that, at 6 weeks after cell culturing, while there was no statistical difference in the osteocalcin (OC) activity between the cells grown on PCL and PLGA films, PCL showed much less alkaline phosphatase activity and mineralization of the cells.

Since it was previously shown[11] that all of the e-spun PCL, PCL/CaCO$_3$, and PCL/HAp fiber mats supported much better adhesion and proliferation of SaOS-2 than the corresponding films and TCPS, and among the various fibrous scaffolds investigated, the PCL/1.0HAp fiber mat exhibited the highest ALP activity, this study aimed at investigating whether PCL and, particularly, the PCL/HAp composite in the form of e-spun fiber mats could support osteogenic differentiation of MC3T3-E1. The potential for use of the PCL and PCL/HAp fiber mats as bone scaffolds was thoroughly evaluated in terms of the attachment, proliferation, differentiation, and subsequent mineralization of MC3T3-E1 that were seeded or cultured on their surfaces. Comparisons were made with the cells that were seeded or cultured on TCPS.

2. Experimental Procedures

2.1. Materials. Materials used in the fabrication of the fibrous scaffolds were polycaprolactone (PCL; $M_n = 80\,000$ g mol^{-1}; Aldrich), dichloromethane (DCM; Carlo Erba), *N,N*-dimethylformamide (DMF; Lab-Scan (Asia)), and hydroxyapatite powder (HAp; synthesized following the method proposed by Shih et al.[25]). After hydrolysis from dicalcium phosphate dihydrate (CaHPO$_4$·2H$_2$O; Fluka Chemika), the HAp powder was annealed at 800 °C for 4 h in air. The obtained HAp powder was characterized by a Rigaku Rint2000 wide-angle X-ray diffractometer (WAXD) with monochromated Cu Kα radiation ($\lambda = 1.54$ Å), which confirmed the formation of HAp.[22] The mean size of the as-synthesized HAp powder as analyzed by a JEOL JSM 5410LV scanning electron microscope was 234 ± 68 nm.[22]

2.2. Preparation and Characterization of Fibrous Scaffolds. E-spun PCL and PCL/HAp fibrous scaffolds (hereafter denoted as PCL-FS and PCL/HAp-FS, respectively) were prepared by e-spinning from a neat 12% w/v PCL solution in 50:50 v/v DCM/DMF or the same PCL solution that contained 1% w/v HAp powder. To ensure a good dispersion of HAp particles within the resulting PCL/HAp suspension, the particles and PCL powder were first premixed under mechanical stirring in DMF. After a certain period of time, DCM, a good solvent for PCL, was added. The mixture was stirred until the PCL powder dissolved completely, and it was subsequently sonicated prior to e-spinning.

The as-prepared PCL solution or the as-prepared PCL/HAp suspension was contained in a glass syringe, the open end of which was

connected to a blunt gauge-20 stainless steel hypodermic needle (o.d. = 0.91 mm) used as the nozzle. An Al sheet wrapped around a rotating cylinder (width and o.d. of the cylinder ≈ 15 cm; rotational speed ≈ 50 rpm) was used as the collector. The distance from the tip of the needle to the surface of the Al sheet defining the collection distance was fixed at 10 cm. A gamma high-voltage research D-ES30PN/M692 power supply was used to generate a high dc potential (i.e., 21 kV). The emitting electrode of positive polarity was connected to the needle, while the grounding one was connected to the collector. The feed rate of the solution/suspension was controlled at ~1 mL h^{-1} by means of a Kd Scientific syringe pump.

E-spinning of the as-prepared solution/suspension was carried out continuously for 10 h. The thickness of the obtained PCL and PCL/HAp fibrous scaffolds was ~130 μm. Morphological appearance and size of the individual fibers of the scaffolds were examined by SEM. At least 100 readings of the fiber diameters from at least five SEM images were statistically analyzed using SemAphore 4.0 software, from which the arithmetic mean values of the individual fibers in the PCL and PCL/HAp fibrous scaffolds were determined to be 0.95 and 1.26 μm, respectively.[22] Fibrous scaffolds were dried in vacuo at 40 °C overnight to remove as much solvent as possible.

2.3. Cell Culturing and Cell Seeding. Mouse calvaria-derived, pre-osteoblastic cells (MC3T3-E1; ATCC CRL-2593) were cultured as monolayers in minimum essential medium with Earle's Balanced Salts (MEM; Hyclone), supplemented by 10% fetal bovine serum (FBS; BIOCHROM AG), 1% L-glutamine (Invitrogen Corp.), and a 1% antibiotic and antimycotic formulation (containing penicillin G sodium, streptomycin sulfate, and amphopericin B (Invitrogen Corp.)). The medium was changed every other day, and the cultures were maintained at 37 °C in a humidified atmosphere containing 5% CO$_2$. Each scaffold was cut into circular discs (~15 mm in diameter), and the disc specimens were placed in wells of a 24-well TCPS (Corning), which was later sterilized in 70% ethanol for 60 min. The specimens were then washed with autoclaved deionized water and subsequently immersed in MEM overnight. To ensure a complete contact between each specimen and the bottom of each well, a metal ring (~12 mm in diameter) was placed on top of the specimen. MC3T3-E1 from the cultures were trypsinized (0.25% trypsin containing 1 mM EDTA (Invitrogen Crop.)), counted by a hemacytometer (Hausser Scientific), and seeded at a density of ~36 000 cells cm^{-2} on the scaffold specimens and empty wells of a TCPS (i.e., positive control).

For the attachment study, cells were cultured in the same medium as stated previously. For the proliferation study, cells were cultured in MEM supplemented by 2% FBS, 1% L-glutamine, and 1% antibiotic/antimycotic. For other studies, cells were cultured in MEM supplemented by 10% FBS, 1% l-glutamine, and 1% antibiotic/antimycotic for the first 5 days, and after that the cells were cultured in the same medium in the presence of 5 mM glycerol-2-phosphate disodium salt hydrate (β-glycerophosphate; Sigma) and 50 μg mL^{-1} l-ascorbic acid (Sigma).

2.4. Cell Attachment and Cell Proliferation. For the attachment study, the cells were allowed to attach on the fibrous scaffold specimens and empty wells of a TCPS for 1, 4, and 16 h. At each time point, the number of the attached cells was quantified by a 3-(4,5-dimethylthiazol-2-yl)-2,5-diphenyl-tetrazolium bromide (MTT; Sigma-Aldrich) assay. Each specimen was rinsed with phosphate buffered saline (PBS; Sigma-Aldrich) to remove unattached cells prior to the MTT assay. Since no studies related to the expression of attachment proteins or the strength of the attached cells were carried out, this evaluation only served as the qualitative measure of the cell attachment study. For the proliferation study, the cells were first allowed to attach on the specimens and empty wells of a TCPS for 16 h. The number of the proliferated cells was determined by MTT assay on days 1, 2, and 3 after cell culturing. The morphology of the cells during the attachment and proliferation periods was observed by SEM.

2.5. Quantification of Viable Cells (MTT Assay). The MTT assay is based on the reduction of the yellow tetrazolium salt to purple
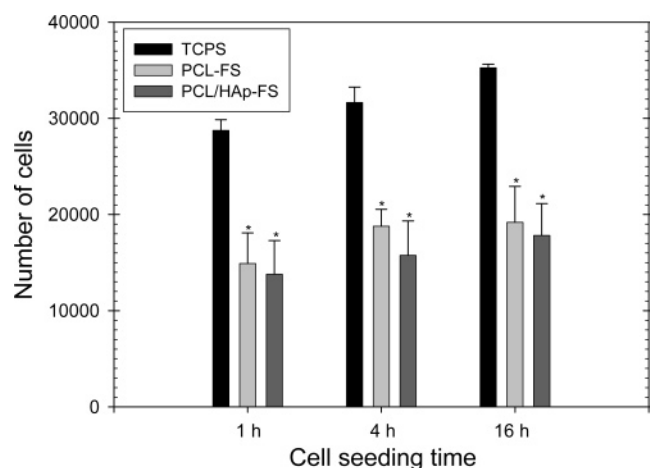
Figure 1. Attachment of MC3T3-E1 that were seeded on the surfaces of TCPS, PCL-FS, and PCL/HAp-FS as a function of cell seeding time. *Significant at $p < 0.05$ with respect to TCPS.

formazan crystals by dehydrogenase enzymes secreted from the mitochondria of metabolically active cells. The amount of purple formazan crystals formed is proportional to the number of viable cells. First, each cell-cultured specimen was incubated at 37 °C for 1 h with a 250 μL/well MTT solution at 0.5 mg mL^{-1} without Phenol Red. After incubation, the MTT solution was removed. A buffer solution containing dimethylsulfoxide (DMSO; Carlo Erba) (900 μL/well) and glycine buffer (pH = 10) (125 μL/well) was added into each well to dissolve the formazan crystals. After 10 min of rotary agitation, each sample solution was then transferred into a cuvette and placed in a Thermo-spectronic Genesis10 UV−vis spectrophotometer, from which the absorbance at 540 nm representing the number of viable cells was measured. The absorbance intensity and number of viable cells were fitted well with a linear regression line (see Figure 1 in the Supporting Information), and this calibration curve was used to arrive at the number of cells from the observed UV absorbance values.

2.6. Morphological Observation of Cultured Cells. After removal of the culture medium, each cell-cultured fibrous scaffold was rinsed with PBS twice, and the cells were then fixed with 3% glutaraldehyde solution, which was diluted from a 50% glutaraldehyde solution (Electron Microscopy Science) with PBS, at 500 μL/well. After 30 min, it was rinsed again with PBS. After cell fixation, the specimen was dehydrated in an ethanol solution of varying concentrations (i.e., 30, 50, 70, 90, and 100%, respectively) for ~2 min at each concentration. It was then dried in 100% hexamethyldisilazane (HMDS; Sigma) for 5 min and later dried in air after the removal of HMDS. After being completely dried, the specimen was mounted on a SEM stub, coated with gold, and observed by SEM. For comparison, the morphology of the cells that were seeded or cultured on a glass substrate (cover glass slide, 12 mm in diameter; Menzel) was also investigated.

2.7. Alkaline Phosphatase Analysis. MC3T3-E1 were cultured on the fibrous scaffolds and empty wells of a TCPS for 1, 2, 3, 5, and 10 day(s) to observe ALP activity. Each specimen was rinsed with PBS after removal of the culture medium. Alkaline lysis buffer (10 mM Tris-HCl, 2 mM MgCl$_2$, 0.1% Triton-X100, pH 10) (100 μL/well) was added, and the specimen was scrapped and then frozen at −20 °C for at least 30 min prior to the next step. An aqueous solution of 2 mg mL^{-1} p-nitrophenyl phosphate (PNPP; Zymed Laboratories) mixed with 0.1 M aminopropanol (10 μL/well) in 2 mM MgCl$_2$ (100 μL/well) having a pH of 10.5 was prepared and added into the specimen. It was then incubated at 37 °C for 25 min. The reaction was stopped by the

addition of 0.9 mL/well of 50 mM NaOH, and the extracted solution was transferred to a cuvette and placed in the UV−vis spectropho-tometer, from which the absorbance at 410 nm was measured. The amount of ALP was then calculated against a standard curve. To determine the ALP activity, the amount of ALP had to be normalized by the amount of total proteins synthesized. In the protein assay, each specimen was treated in the same manner as in the ALP assay up to the point where it was frozen. After freezing, a bicinchoninic acid (BCA; Pierce Biotechnology) solution was added into the specimen. It was subsequently incubated at 37 °C for 25 min. The absorbance of the medium solution was then measured at 562 nm by the UV−vis spectrophotometer, and the amount of the total proteins was calculated against a standard curve.

2.8. Reverse Transcription-Polymerase Chain Reaction (RT-PCR) Analysis. MC3T3-E1 were cultured on the fibrous scaffolds and empty wells of a TCPS for 14 days. RNA, extracted by Tri Reagent (Molecular Research Center), was harvested and pooled from four wells for each type of specimen. Chloroform (200 μL) was added to the homogenized specimens to extract RNA, followed by precipitation using 500 μL of isopropyl alcohol (Sigma). RNA pellets were washed with 70% ethanol and were dissolved in 15 μL of nuclease-free water (Promega). RNA yields were evaluated by the UV−vis spectropho-tometer based on absorbance at 260 nm. First strand DNA was reverse transcribed from 1 μg of total RNA using a RT kit (ImProm-II Reserve Transcription System, Promega). For the amplification in PCR, the PCR mixture consisted of 1 μL of cDNA, sense primer, antisense primer, and reagent of the PCR kit (Tag DNA Polymerase, Qiagen). The PCR oligonucleotide primers for OC[26] and glyceraldehyde-3-phosphate dehydrogenase (GAPDH)[27] (used as an internal control) are shown in Table 1. Twenty-eight cycles were used to amplify both genes. The PCR products were analyzed by separation on 1.8% agarose (Usb) gel using electrophoresis (Power Pac Junior, Bio-Rad) and visualized with ethidium bromide (EtBr; Bio-Rad) staining. The stained bands were photographed under UV light, and the intensity was quantified with Scion Image Software.

2.9. Western Blot Analysis. MC3T3-E1 were cultured on the fibrous scaffolds and empty wells of a TCPS for 21 days. The cultured medium for each type of specimen was collected and lyophilized. Lyophilized medium was dissolved with sample buffer (2% SDS, 10% glycerol, 250 mM Tris-HCl, and 0.005% Bromophenol Blue). The supernatant was collected and was subjected to SDS-PAGE under non-reducing conditions, followed by transferring to the PVDF membrane (Millipore). The membrane was blocked by incubating in a blocking solution containing 5% skim milk (Difco, BD) and 0.1% TWEEN 20 (Fluka Chemika) for 3 h. The membrane was then incubated and shaken in a primary antibody solution (mouse OC antibody, SC-18322; Santa Cruz Biotechnology), which was diluted in a blocking solution at an antibody to blocking solution ratio of 1:200 v/v for 1 h. The membrane was washed with PBS before being incubated and shaken in a secondary antibody solution (anti-goat IgG, B7014; Biotin Conjugate, Sigma) at an antibody to blocking solution ratio of 1:2000 v/v for 20 min. The membrane was again washed with PBS. The membrane was incubated and shaken in a streptavidin horseradish peroxidase (HRP) conjugate (Zymed) solution at a streptavidin HRP to blocking solution ratio of 1:500 v/v for 30 min and washed with PBS. All incubations were carried out at room temperature. The membrane was then immersed in 1 mL of SuperSignal West Pico chemiluminescent reagent (Pierce). The signal was captured with a CL-XPosure film (Pierce).

2.10. Mineralization Analysis and Bone Nodule Visualization. Calcium deposition was quantified by Alizarin Red S (i.e., an anthraquinone derivative) staining. MC3T3-E1 were cultured on the

Table 1. Primers for PCR Amplification

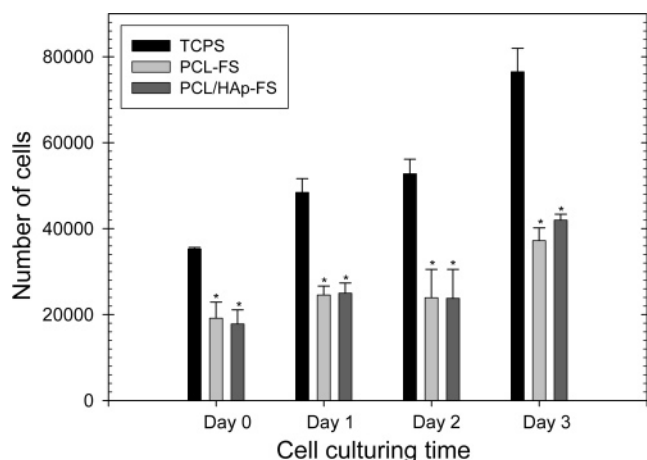| gene	primer sequence	size (position)
OC	F: 5′CTTGGGTTCTGACTGGGTGT3′R: 5′AGGGAGGATCAAGTCCCG3′	525 bp
GAPDH	F: 5′ACTTTGTCAAGCTCATTTCC3′R: 5′TGCAGCGAACTTTATTGATG3′	269 bp

Figure 2. Proliferation of MC3T3-E1 that were cultured on the surfaces of TCPS, PCL-FS, and PCL/HAp-FS as a function of the time in culture. *Significant at $p < 0.05$ with respect to TCPS.

fibrous scaffolds and empty wells of a TCPS for 14 and 21 days, after which the cells were fixed with cold methanol for 10 min and washed with deionized water prior to immersion for 3 min in 370 μL of 1% Alizarin Red S (Sigma) solution dissolved in 1:100 (v/v) ammonium hydroxide/water mixture. Each stained specimen was washed several times with deionized water and air-dried at room temperature. Calcium forms an Alizarin Red S−calcium complex in a chelating process. The stained specimen was photographed and the redness, signifying the amount of calcium deposition, was quantified by Scion Image Software. The intensity for each specimen was subtracted by the intensity of the blank specimen. Bone nodule formation of the cells that were cultured on the fibrous scaffolds on day 21 after cell culturing was observed by SEM, and the presence of calcium on the cell-cultured specimens was characterized by energy dispersive X-ray spectroscopy (EDS; Link ISIS series 300) mapping.

2.11. Statistical Analysis. All values were expressed as mean ± standard deviation. Statistical analysis was carried out by the one-way analysis of variance (one-way ANOVA) and Scheffe's post hoc test in SPSS (SPSS). The statistical difference between two sets of data was considered when $p < 0.05$.

3. Results

3.1. Cell Attachment and Cell Proliferation. Figure 1 shows the attachment of MC3T3-E1 on surfaces of TCPS, PCL-FS, and PCL/HAp-FS at 1, 4, and 16 h after cell seeding in terms of the number of cells attached. On TCPS, the number of the attached cells increased from ∼80% at 1 h after cell seeding to ∼98% at 16 h after cell seeding, based on the initial number of cells seeded (36 000 cells cm^{-2}). In comparison with that on TCPS, the attachment of the cells on PCL-FS and PCL/HAp-FS was significantly lower. Specifically, the number of cells attached on these fibrous scaffolds was only ∼50% in comparison to that on TCPS at any given time point. Between both types of fibrous scaffolds, the number of MC3T3-E1 attached on PCL-FS was slightly better than that on PCL/HAp-FS.

Figure 2 shows the proliferation of MC3T3-E1 on the surfaces of TCPS, PCL-FS, and PCL/HAp-FS on days 1−3 after cell culturing in terms of the number of viable cells. For this study, the cells were first allowed to attach on the substrates for 16 h (denoted as day 0 on the figure). Again, at the initial attachment period of 16 h, the number of cells attached on TCPS was ∼98 and ∼50% on both types of fibrous scaffolds. On TCPS, the number of cells increased from ∼135% on day 1 after cell culturing to ∼212% (i.e., an increase of about 2-fold from the initial number of cells seeded) on day 3 after cell culturing. In

comparison with that on TCPS, the proliferation of the cells on PCL-FS and PCL/HAp-FS was significantly lower. Specifically, the number of cells proliferated on these fibrous scaffolds, at any given time point, was ∼45 to ∼55% in comparison to that on TCPS. Between both types of fibrous scaffolds, the proliferation of the cells on PCL-FS was comparable to that on PCL/HAp-FS on days 1 and 2 after cell culturing, but that on PCL/HAp-FS was slightly greater than that on PCL-FS on day 3 after cell culturing.
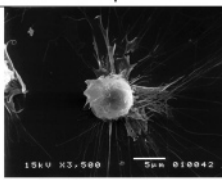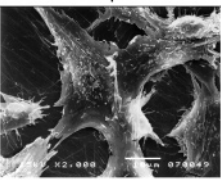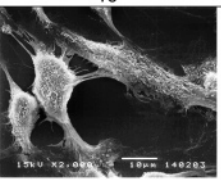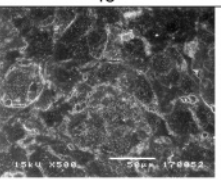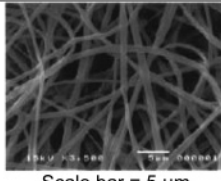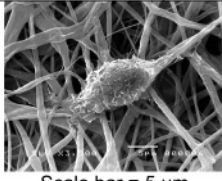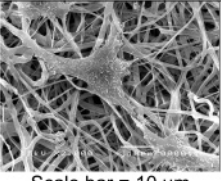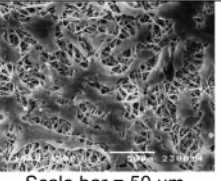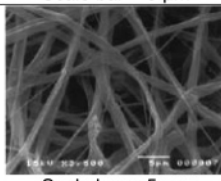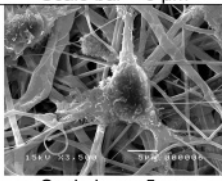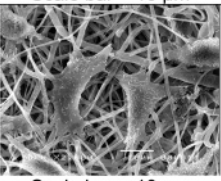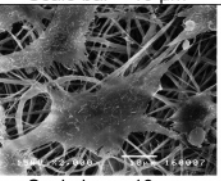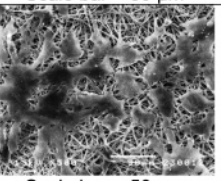
The lesser number of cells in the proliferation period on both types of the fibrous scaffolds in comparison to that on TCPS could be due to the lesser number of cells that were able to attach on the rough and hydrophobic surface of the fibrous scaffolds in comparison to the smoother and more hydrophilic surface of TCPS. Despite the disparity in the number of cells attached on the various substrates at the initial attachment period of 16 h, the percentage of the ratio between the number of cells at any given time point to the number of cells initially attached on any given substrate was found to increase in a similar manner, with PCL/HAp-FS exhibiting the greatest value on day 3 after cell culturing. Specifically, on days 1−3 after cell culturing, such percentage values for TCPS were 137, 150, and 217%, respectively, those for PCL-FS were 128, 125, and 194%, respectively, and those for PCL/HAp-FS were 140, 134, and 235%, respectively. Apparently, despite the lower number of attached cells, the fibrous scaffolds were able to support the proliferation of MC3T3-E1 at essentially similar levels to that of the cells on TCPS, with the cells grown on PCL/HAp-FS showing the greatest proliferation rate on day 3 after the initial attachment period of 16 h.

Table 2 shows selected SEM images of MC3T3-E1 that were either seeded or cultured on the surfaces of glass, PCL-FS, and PCL/HAp-FS at different time points. The use of glass as the control instead of TCPS was due to the ease of taking the samples to the SEM observation. These images provided snapshots in time that revealed the morphology of the cells and interaction between the cells and the tested surfaces. At 1 h after cell seeding, the majority of the cells on the glass surface was still rounded, but a closer examination around the edge of the cells revealed an evidence of filopodia. At 4 h after cell seeding, the majority of the cells began to extend their cytoplasm over the glass surface, an evidence of the ability of the cells to attach on the surface. At 16 h after cell seeding, expansion of the cytoplasm of the majority of the cells was evident. On day 2 after cell culturing, the cells proliferated to cover ∼60−70% of the glass surface.

Even at 1 h after cell seeding, the majority of the cells on the PCL-FS surface showed an evidence of the extension of their cytoplasm on the fibrous surface, while the majority of the cells on the PCL/HAp-FS surface did so to a greater extent, suggesting that the cells prefer the fibrous surfaces of PCL-FS and PCL/HAp-FS over that of the glass. The complete expansion of the cytoplasm of the majority of the cells on the surfaces of the fibrous scaffolds was evident at 4 and 16 h after cell seeding. On day 2 after cell culturing, the cells proliferated to cover ∼40−50% of their surfaces.

3.2. ALP Activity. The ALP activity of MC3T3-E1 that were cultured on TCPS, PCL-FS, and PCL/HAp-FS was monitored on days 1, 2, 3, 5, and 10 after cell culturing (see Figure 3). Apparently, the amount of ALP synthesized by the cells that were cultured on TCPS increased with the initial increase in the time in culture between days 1 and 3, reached a maximum level on day 3, and decreased with a further increase in the time in culture after day 3. On the other hand, the amount of

Table 2. Selected SEM Images of Cultured Specimens (i.e., Glass (Control), PCL-FS, and PCL/HAp-FS) at Various Time Points after MC3T3-E1 Were Seeded or Cultured on Their Surfaces

Substrate	As-spun	1	4	16	48
			Time in culture (h)		
Glass	n/a	Scale bar = 5 μm	Scale bar = 10 μm	Scale bar = 10 μm	Scale bar = 50 μm
PCL-FS	Scale bar = 5 μm	Scale bar = 5 μm	Scale bar = 10 μm	Scale bar = 10 μm	Scale bar = 50 μm
PCL/HAp-FS	Scale bar = 5 μm	Scale bar = 5 μm	Scale bar = 10 μm	Scale bar = 10 μm	Scale bar = 50 μm

ALP synthesized by the cells on PCL/HAp-FS also increased with the initial increase in the time in culture between days 1 and 5, reached a maximum level on day 5, and decreased significantly on day 10. Interestingly, on day 5, the amount of ALP observed on PCL/HAp-FS was slightly lower than that observed on TCPS. Since ALP is not an exclusive protein synthesized by osteoblasts as it is also found in tissues of such organs as kidneys, small intestines, and placenta,[27] the presence of ALP of MC3T3-E1 that were cultured on these substrates could not be used as the sole marker to confirm the osteoblastic phenotype of the cells.

3.3. RT-PCR Analysis. Gel electrophoresis following RT-PCR using the designed primers shown in Table 1 revealed the snapshot in time for the expression of the OC gene, an osteoblast-specific gene,[28−30] of MC3T3-E1 on day 14 after the cells were cultured on TCPS, PCL-FS, and PCL/HAp-FS. The expression of the GAPDH gene was used as an internal control. The amount of both genes was semiquantified by the band intensities shown in Figure 4a (i.e., the top panel shows the

band intensities of GAPDH gene expression, while the bottom panel shows those of OC gene expression). Evidently, the expression of the GAPDH gene for the cells that were cultured on different substrates was similar, while that of the OC gene for the cells that were cultured on PCL/HAp-FS showed the greatest intensity, followed by that for the cells that were cultured on PCL-FS and TCPS, respectively. Normalization of the band intensities of the OC gene to those of the GAPDH gene revealed more evidence on the relative amount of the OC gene expressed in the cells when they were cultured on different surfaces (see Figure 4b). Apparently, OC gene expression in the cells that were grown on PCL/HAp-FS was significantly greater than those grown on both PCL-FS and TCPS, while that of the cells that were grown on PCL-FS was significantly
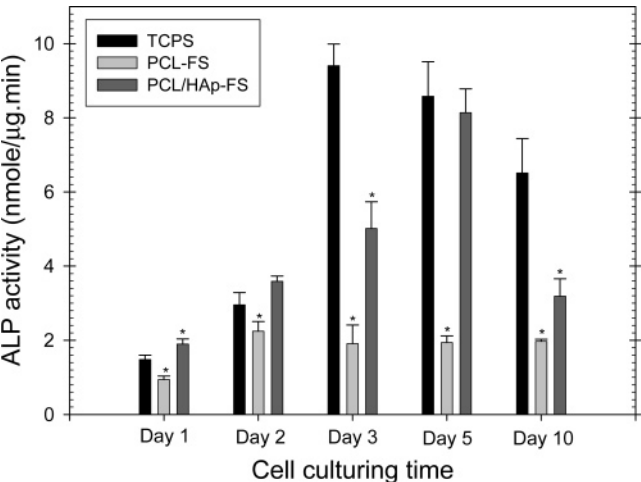

Figure 3. ALP activity of MC3T3-E1 that were cultured on the surfaces of TCPS, PCL-FS, and PCL/HAp-FS at various time points after cell culturing. *Significant at $p < 0.05$ with respect to TCPS.
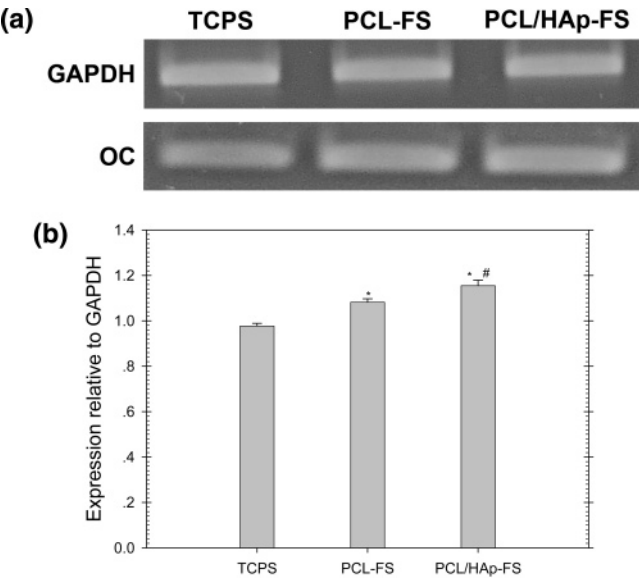

Figure 4. Expression of OC gene in MC3T3-E1 on day 14 after being cultured on the surfaces of TCPS, PCL-FS, and PCL/HAp-FS. Intensity of each band was semiquantified (a) and normalized (b) with that of GAPDH. *Significant at $p < 0.05$ with respect to TCPS. #-Significant at $p < 0.05$ with respect to PCL-FS.
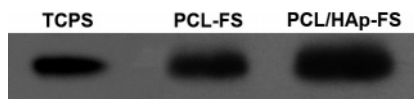
Figure 5. Western blot analysis for expression of OC by MC3T3-E1 on day 21 after being cultured on the surfaces of TCPS, PCL-FS, and PCL/HAp-FS. Intensity of each band was semiquantified.
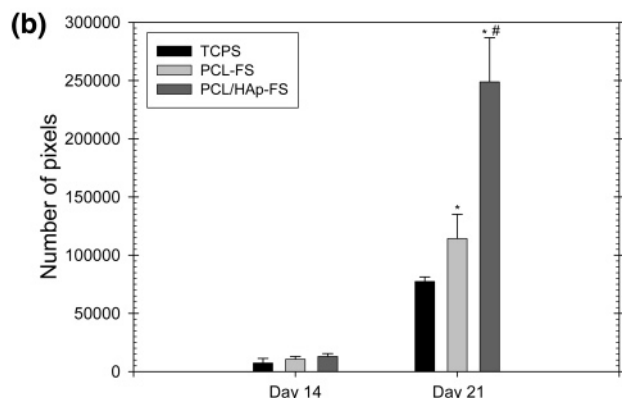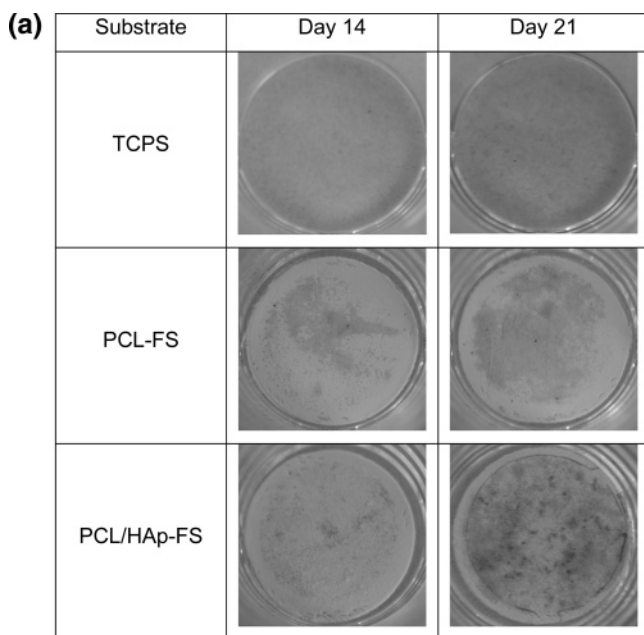

Figure 6. Alizarin Red S staining for mineralization assessment of MC3T3-E1 on days 14 and 21 after being cultured on the surfaces of TCPS, PCL-FS, and PCL/HAp-FS: (a) photographic images of stained specimens and (b) corresponding analysis for the number of red pixels observed for each fibrous scaffolding specimen. *Significant at $p < 0.05$ with respect to TCPS. #Significant at $p < 0.05$ with respect to PCL-FS.

Figure 7. Selected SEM images (magnification = 750×; scale bar = 10 μm) of cultured fibrous scaffolding specimens (i.e., (a) PCL-FS and (b) PCL/HAp-FS) on day 21 after MC3T3-E1 were cultured on their surfaces.

greater than those grown on TCPS. The expression of the OC gene in these cells confirmed the osteoblastic phenotype of the cells.

3.4. Western Blot Analysis. The presence of the OC gene in MC3T3-E1 that were cultured on the surfaces of TCPS, PCL-FS, and PCL/HAp-FS was evident on day 14 after cell culturing. To verify the actual production of OC, a non-collagenous protein specifically secreted by osteoblasts and thought to play a role in mineralization and calcium ion homeostasis,[28–30] Western blot analysis was carried out. Figure 5 shows band intensities of OC expression after the cells were cultured on the surfaces of these substrates for 21 days. On the basis of the intensities of the bands shown in Figure 5, the cells that were cultured on PCL/HAp-FS showed the greatest amount of synthesized OC, as reflected by the greatest intensity of the band, than those
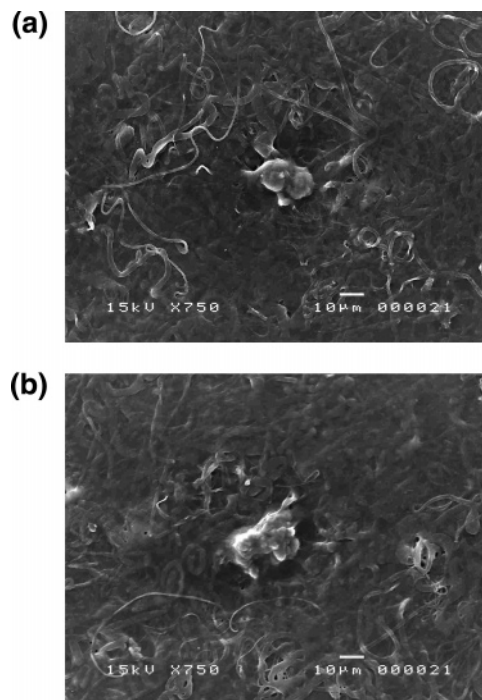
cultured on PCL-FS and TCPS, respectively. Similar findings were obtained with dot blot analysis (see the additional experiment in the Supporting Information).

3.5. Bone Nodule Formation. Bone nodule formation is one of the markers specific to bone cell differentiation.[28–30] Alizarin Red S staining was used to characterize the bone nodule formation of MC3T3-E1 that were cultured on the surfaces of TCPS, PCL-FS, and PCL/HAp-FS for 14 and 21 days, while SEM visualization and EDS mapping were used to characterize the cultured specimens for mineralization on day 21 after cell culturing.

Figure 6a shows photographic images of Alizarin Red S staining of cells cultured on the different surfaces on days 14 and 21. In the presence of calcium, the staining product (i.e., an Alizarin Red S-calcium chelating product) appeared red. Quantitative analysis of the results shown in Figure 6a was carried out by determining the number of red pixels observed in each image using image analytical software, and the results of the analysis are shown in Figure 6b. On day 14 after cell culturing, the amount of red pixels observed for PCL/HAp-FS was the greatest, followed by that observed for PCL-FS and TCPS, respectively. A marked increase in the amount of the red pixels was observed for all of the substrates investigated on day 21. Evidently, the cells that were cultured on the surface of PCL/HAp-FS showed the most positive staining for calcium deposition, followed by those on the surfaces of PCL-FS and TCPS, respectively.

Mineralization of MC3T3-E1 that were cultured on PCL-FS and PCL/HAp-FS on day 21 was further characterized by SEM and EDS imaging. Figure 7 shows selected SEM images of cell-cultured fibrous scaffolding specimens. Traces of individual PCL fibers were still intact in these images, but after 21 days in cell culturing, remnants of solid residues were evident in the pores as well as on the surface of the individual fibers, possibly evidence of the protein matrix residues produced by the cells. As compared to the cells that were cultured on the surfaces of
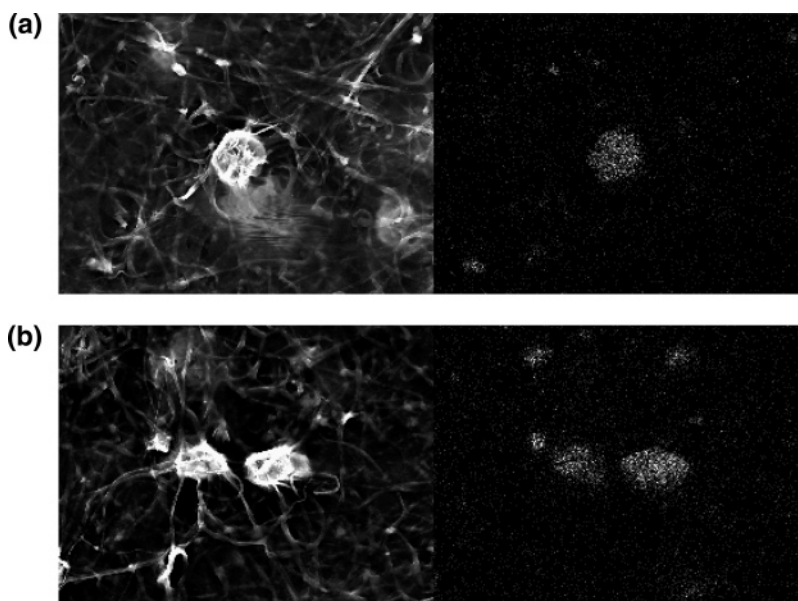
Figure 8. Selected SEM images and their corresponding EDS images for calcium of cultured fibrous scaffolding specimens (i.e., (a) PCL-FS and (b) PCL/HAp-FS) on day 21 after MC3T3-E1 were cultured on their surfaces.

these fibrous scaffolds at earlier time points (see Table 2), the formation of nodules was evident on the surfaces of the cells. Apparently, on the majority of the SEM images observed, the number of nodules on the surface of the cells that were cultured on PCL/HAp-FS was greater than that on the PCL-FS counterpart. The formation of bone nodules was confirmed further by EDS mapping. Figure 8 shows selected SEM images and their corresponding EDS images of cell-cultured fibrous scaffolding specimens (i.e., similar to those shown in Figure 7 but without the gold coating). Elemental calcium was clearly observed on the surfaces of the cells, the result that confirmed the full osteoblastic phenotype of MC3T3-E1 when they were cultured on the surfaces of these fibrous scaffolds.

4. Discussion

In our previous report,[11] the e-spun PCL fiber mats and the ones that contained either $CaCO_3$ or HAp nanoparticles (i.e., $PCL/CaCO_3$ and PCL/HAp) exhibited much better support for the adhesion and proliferation of human osteogenic sarcoma cells (SaOS-2) than the corresponding solvent-cast films and TCPS, and among the various fibrous scaffolds investigated, the ones containing 1.0 wt % HAp (i.e., PCL/1.0HAp) showed the greatest ALP activity. On the contrary, different surface microtopographies of commercially pure titanium (cpTi) discs (i.e., grooved vs roughened) only affected the expression of transcription factor Cbfa1 and bone sialoprotein (BSPII) genes and subsequent mineralization of osteoblasts (i.e., UMR-106−-01-BSP and primary rat calvarial osteoblasts) that were grown on them, but they did not affect the attachment nor the proliferation of the cells.[31]

In contrast to what was observed in our previous report,[11] the ability of the e-spun PCL fiber mats (i.e., PCL-FS) and the ones containing 1.0 wt % HAp (i.e., PCL/HAp-FS) in supporting the adhesion and proliferation of mouse calvaria-derived, pre-osteoblastic cells, MC3T3-E1, was less than TCPS. Specifically, the number of cells attached and proliferated on the fibrous scaffolds at any given time point was ∼50% in comparison to that on TCPS. The lesser number of MC3T3-E1 attached on both the fibrous scaffolds could be due to the hydrophobicity of the scaffolds in comparison with TCPS since MC3T3-E1

were reported to adhere better on a hydrophilic surface.[32] However, despite the lesser number of attached cells, both the fibrous scaffolds were able to support the proliferation of MC3T3-E1 at similar levels to that of the cells on TCPS, with the cells growing on PCL/HAp-FS showing the greatest proliferation rate on day 3 after the initial attachment period of 16 h. In this work, we paid particular interest to the ability of the fibrous scaffolds in supporting the full osteogenic differentiation of MC3T3-E1.

Analyses of the expression patterns of regulating genes and bone-related proteins revealed three sequential stages during the proliferation and differentiation of MC3T3-E1 including proliferation, bone matrix formation and maturation, and mineralization.[28,30] There exist two restriction points to which the cells can progress but cannot develop further without further signals: the first when proliferation is down-regulated and gene expression associated with the extracellular matrix maturation is induced and the second when mineralization occurs.[28,30] Initially, actively proliferating cells produce a fibronectin/type I collagen,[28] type I collagen/TGF-β1, or fibronectin/osteonectin extracellular matrix.[30] During the bone matrix formation and maturation period, the expressions of type I collagen, fibronectin, TGF-β1, and osteonectin were evident.[30] The down-regulation of the proliferation period and the up-regulation of the matrix maturation and mineralization are marked by a temporal sequence of events in which there is an enhanced expression of ALP immediately following the proliferation period and an increased expression of osteopontin and OC at the onset of mineralization.[28] However, it was also suggested that ALP is highly expressed during the early matrix formation and maturation period, followed by a decrease in its activity, and during the mineralization period, the expression of OC and the number of nodules are high.[30]

Although its exact function is not known, ALP is believed to provide inorganic phosphate for mineralization.[24] On the basis of the results shown in Figure 2, the number of cells proliferated on TCPS was ∼212% based on the initial number of cells seeded (36 000 cells cm^{-2}). Assuming that the production of ALP should begin as soon as cell-to-cell contacts were established (viz. the cessation of the proliferation period),[28] the amount of ALP synthesized by the cells on TCPS should be the greatest

at any given time point. With regards to the fibrous scaffolds, since the number of cells proliferated on these surfaces was about the same (i.e., between ~53 and 103% for PCL-FS and between ~50 and 117% for PCL/HAp-FS, based on the initial number of cells seeded (36 000 cells cm^{-2}), for the cells that were cultured between 1 and 3 days), it is expected that the amounts of ALP synthesized by the cells that were cultured on these fibrous scaffolds should be at similar levels. This is, however, not the case, since the cells on PCL/HAp-FS exhibited much greater ALP activity than PCL-FS, and the amount of ALP synthesized by the cells on PCL/HAp-FS on day 5 was close to that observed on TCPS. The enhancement in the ALP activity of the cells grown on the surface of PCL/HAp-FS should be due to the presence of HAp that was shown to promote the ALP activity of human pulp fibroblasts.[27]

Because of the much greater number of MC3T3-E1 attached and proliferated on TCPS, the ALP activity of the cells grown on TCPS reached a maximal value on day 3 after cell culturing, while that of the cells grown on PCL/HAp-FS did so on day 5. Interestingly, the ALP activity of the cells grown on PCL-FS was the lowest at any given time point, despite the relatively greater number of cells attached on its surface than that on the PCL/HAp-FS counterpart. This observation is in line with earlier reports by Calvert et al.[23,24] In their first report,[23] negative staining for ALP was observed for the bone marrow stromal cells (New Zealand white rabbits) that had been grown on a PCL coated glass surface for 10 days, while those grown on the uncoated glass surface exhibited the highest staining for ALP. In their subsequent work,[24] the expression of both the ALP genes (on day 4 after cell culturing) and the ALP (at 6 weeks after cell culturing) of MC3T3-E1 grown on the PCL coated glass surface was markedly less than that on the uncoated glass surface.

The fastest development in the ALP activity of the cells grown on TCPS was obviously due to the greatest number of cells grown on its surface. It is likely that the up-regulation for the production of ALP was triggered by cellular contacts (when the cells reached the confluence) and/or by the expression of ample amounts of early matrix proteins (e.g., type I collagen, fibronectin, and/or TGF-β1).[28-30] On days 1 and 2, the greater expression of ALP of the cells grown on PCL/HAp-FS in comparison to that on TCPS should be a result of the presence of HAp that helps trigger the expression of ALP,[27] while the delay in its maximal expression, in comparison with that on TCPS, should be due to the lower number of cells on day 3 such that an additional 2 days were required for the cells to proliferate more, leading to the marked increase in the total amount of ALP synthesized. The decrease in the ALP activity, after the maximal expression of ALP on day 3 for the cells grown on TCPS and on day 5 for those grown on PCL/HAp-FS, with a further increase in the culturing time was in general agreement with that observed by Choi et al.[30]

The greater expression for both the OC gene and the OC protein on days 14 and 21, respectively, of MC3T3-E1 after being cultured on the surface of PCL/HAp-FS than that on the surfaces of PCL-FS and TCPS was evident. OC, or γ-carboxy-glutamic acid or Gla protein, is an abundant Ca^{2+} binding protein commonly found in the organic matrix of bone, dentin, and other mineralized tissues.[29] It constitutes ~2−3% of the total protein content found in bone.[24,33] OC is postulated to play an important role in mineralization by its ability to bind both calcium and HAp,[29] and it was reported that coating the glass surface with HAp and serum protein increased the ALP activity, promoted the proliferation rate, and enhanced the mineralized extracellular matrix of MC3T3-E1, perhaps through increased adsorption of fibronectin,[34] which is one of the proteins secreted by proliferating cells.[28,30] Because of the observed amounts of both the OC gene and the OC protein for the cells grown on the surfaces of the fibrous scaffolds and TCPS, it is expected that the extent of mineralization should be the greatest for the cells grown on PCL/HAp-FS, followed by that on PCL-FS and TCPS, respectively, which is exactly what was observed here.

5. Conclusion

In the present study, e-spinning was used to fabricate e-spun fiber mats of polycaprolactone (PCL; $M_n = 80\,000$ g mol^{-1}) with or without the presence of HAp nanoparticles from a neat PCL solution (i.e., 12% w/v in 50:50 v/v dichloromethane/N,N-dimethylformamide) or the PCL solution that contained 1% w/v HAp nanoparticles. These e-spun fiber mats (i.e., PCL-FS for the neat e-spun PCL fiber mat and PCL/HAp-FS for the e-spun PCL fiber mat containing HAp nanoparticles) were used as scaffolding materials for the culture of mouse calvaria-derived, pre-osteoblastic cells, MC3T3-E1. Particular interest was paid on whether or not these fibrous scaffolds could support the full osteoblastic phenotype expression of MC3T3-E1. The number of cells attached and proliferated on both types of the fibrous scaffolds at any given time point was ~50%, as compared with that on TCPS, which was used as the positive control. Despite the lower number of cells at early time points, both the fibrous scaffolds were able to support the proliferation of MC3T3-E1 at similar levels to TCPS, with the cells growing on PCL/HAp-FS showing the greatest proliferation rate on day 3 after the initial attachment period of 16 h. Because of the much greater number of cells attached and proliferated on TCPS, the ALP activity of MC3T3-E1 grown on TCPS reached a maximal value on day 3 after cell culturing, while that of the cells grown on PCL/HAp-FS did so on day 5. On the contrary, the ALP activity of the cells grown on PCL-FS was the lowest at any given time point, despite the relatively greater number of cells attached on its surface than that on the PCL/HAp-FS counterpart. MC3T3-E1 cultured on the surface of PCL/HAp-FS exhibited the greatest amount of OC gene on day 14 after cell culturing and the greatest amount of OC protein on day 21 after cell culturing, when compared to those cultured on the surfaces of PCL-FS and TCPS. This translated to the greatest extent of mineralization for the cells grown on the surface of PCL/HAp-FS on day 21, followed by that for the cells grown on PCL-FS and TCPS, respectively.

Supporting Information Available. Additional experiment and results (Figures 1−3). This material is available free of charge via the Internet at http://pubs.acs.org.

References and Notes

(1) Doshi, J.; Reneker, D. H. *J. Electrostat.* **1995**, *35*, 151.
(2) Deitzel, J. M.; Kleinmeyer, J.; Harris, D.; Beck Tan, N. C. *Polymer* **2001**, *42*, 261.
(3) Gibson, P. W.; Schreuder-Gibson, H. L.; Rivin, D. *AIChE J.* **1999**, *45*, 190.
(4) Bergshoef, M. M.; Vancso, G. J. *Adv. Mater.* **1999**, *11*, 1362.
(5) Kim, J. S.; Reneker, D. H. *Polym. Compos.* **1999**, *20*, 124.
(6) Kenawy, E. R.; Bowlin, G. L.; Mansfield, K.; Layman, J.; Simpson, D. G.; Sanders, E. H.; Wnek, G. E. *J. Controlled Release* **2002**, *81*, 57.
(7) (a) Taepaiboon, P.; Rungsardthong, U.; Supaphol, P. *Nanotechnology* **2006**, *17*, 2317. (b) Taepaiboon, P.; Rungsardthong, U.; Supaphol, P. *Nanotechnology* **2007**, *18*, 175102.
(8) Li, W.-J.; Laurencin, C. T.; Caterson, E. J.; Tuan, R. S.; Ko, F. K. *J. Biomed. Mater. Res.* **2002**, *60*, 613.
(9) Teo, W.-E.; He, W.; Ramakrishna, S. *Biotechnol. J.* **2006**, *1*, 918.
(10) Liao, S.; Li, B.; Ma, Z.; Wei, H.; Chan, C.; Ramakrishna, S. *Biomed. Mater.* **2006**, *1*, 45.
(11) Wutticharoenmongkol, P.; Sanchavanakit, N.; Pavasant, P.; Supaphol, P. *J. Nanosci. Nanotechnol.* **2006**, *6*, 514.
(12) Ji, Y.; Ghosh, K.; Shu, X. Z.; Li, B.; Sokolov, J. C.; Prestwich, G. D.; Clark, R. A. F.; Rafailovich, M. H. *Biomaterials* **2006**, *27*, 3782.
(13) Meechaisue, C.; Dubin, R.; Supaphol, P.; Hoven, V. P.; Kohn, J. *J. Biomater. Sci., Polym. Ed.* **2006**, *17*, 1039.
(14) Suwantong, O.; Waleetorncheepsawat, S.; Sanchavanakit, N.; Pavasant, P.; Cheepsunthorn, P.; Bunaprasert, T.; Supaphol, P. *Int. J. Biol. Macromol.* **2007**, *40*, 217.
(15) Sombatmankhong, K.; Sanchavanakit, N.; Pavasant, P.; Supaphol, P. *Polymer* **2007**, *48*, 1419.
(16) Boyan, B. D.; Lohmann, C. H.; Romero, J.; Schwartz, Z. *Clin. Plast. Surg.* **1999**, *26*, 629.
(17) Hutmacher, D. W. *Biomaterials* **2000**, *21*, 2529.
(18) Hutmacher, D. W.; Schantz, T.; Zein, I.; Ng, K. W.; Toeh, S. H.; Tan, K. C. *J. Biomed. Mater. Res.* **2001**, *55*, 203.
(19) Bölgen, N.; Mencelo''lu, Y. Z.; Acatay, K.; Vargel, İ.; Pişkin, E. *J. Biomater. Sci., Polym. Ed.* **2005**, *16*, 1537.
(20) Kim, H. W.; Lee, E. J.; Kim, H. E.; Salih, V.; Knowles, J. C. *Biomaterials* **2005**, *26*, 4395.
(21) Chim, H.; Hutmacher, D. W.; Chou, A. M.; Oliveira, A. L.; Reis, R. L.; Lim, T. C.; Schantz, J.-T. *Intl. J. Oral Maxillofacial Surg.* **2006**, *35*, 928.
(22) Wutticharoenmongkol, P.; Sanchavanakit, N.; Pavasant, P.; Supaphol, P. *Macromol. Biosci.* **2006**, *6*, 70.
(23) Calvert, J. W.; Marra, K. G.; Cook, L.; Kumta, P. M.; DiMilla, P. A.; Weiss, L. E. *J. Biomed. Mater. Res.* **2000**, *52*, 279.
(24) Calvert, J. W.; Chua, W. C.; Gharibjanian, N. A.; Dhar, S.; Evans, G. R. D. *Plast. Reconstr. Surg.* **2005**, *116*, 567.
(25) Shih, W. J.; Chen, Y. F.; Wang, M. C.; Hon, M. H. *J. Cryst. Growth* **2004**, *270*, 211.
(26) Filopodia, http://en.wikipedia.org/wiki/Filopodia.
(27) Tsukamoto, Y.; Fukutani, S.; Mori, M. *J. Mater. Sci.: Mater. Med.* **1992**, *3*, 180.
(28) Owen, T. A.; Aronow, M.; Shalhoub, V.; Barone, L. M.; Wilming, L.; Tassinari, M. S.; Kennedy, M. B.; Pockwinse, S.; Lian, J. B.; Stein, G. S. *J. Cell. Physiol.* **1990**, *143*, 420.
(29) Hauschka, P. V.; Lian, J. B.; Cole, D. E. C.; Gundberg, C. M. *Physiol. Rev.* **1989**, *69*, 990.
(30) Choi, J. Y.; Lee, B. H.; Song, K. B.; Park, R. W.; Kim, I. S.; Sohn, K. Y.; Jo, J. S.; Ryoo, H. M. *J. Cell. Biochem.* **1996**, *61*, 609.
(31) Schneider, G. B.; Perinpanayagam, H.; Clegg, M.; Zaharias, R.; Seabold, D.; Keller, J.; Stanford, C. *J. Dent. Res.* **2003**, *82*, 372.
(32) Xi, J.; Kong, L.; Gao, Y.; Gong, Y.; Zhao, N.; Zhang, X. *J. Biomater. Sci., Polym. Ed.* **2005**, *16*, 1395.
(33) Rammelt, S.; Neumann, M.; Hanisch, U.; Reinstorf, A.; Pompe, W.; Zwipp, H.; Biewener, A. *J. Biomed. Mater. Res.* **2005**, *73*, 284.
(34) El-Ghannam, A.; Ducheyne, P.; Shapiro, I. M. *J. Biomed. Mater. Res.* **1997**, *36*, 167.

BM700451P